Autophagy inhibition potentiates SAHA-mediated apoptosis in glioblastoma cells by accumulation of damaged mitochondria

KOVOORU LOHITESH[1], HEENA SAINI[1], ABHILASHA SRIVASTAVA[1], SUDESHNA MUKHERJEE[1], ANIRUDDHA ROY[2] and RAJDEEP CHOWDHURY[1]

[1]Department of Biological Sciences and [2]Department of Pharmacy, Birla Institute of Technology and Science (BITS), Pilani Campus, Pilani, Rajasthan 333031, India

Received November 9, 2017; Accepted March 23, 2018

DOI: 10.3892/or.2018.6373

Abstract. Glioblastoma multiforme (GBM), often referred to as a grade IV astrocytoma, is the most invasive type of tumor arising from glial cells. The main treatment options for GBM include surgery, radiation and chemotherapy. However, these treatments tend to be only palliative rather than curative. Poor prognosis of GBM is due to its marked resistance to standard therapy. Currently, temozolomide (TMZ), an alkylating agent is used for treatment of GBM. However, GBM cells can repair TMZ-induced DNA damage and therefore diminish the therapeutic efficacy of TMZ. The potential to evade apoptosis by GBM cells accentuates the need to target the non-apoptotic pathway and/or inhibition of pro-survival strategies that contribute to its high resistance to conventional therapies. In recent studies, it has been demonstrated that HDAC inhibitors, such as vorinostat (suberoyl anilide hydroxamic acid; SAHA) can induce autophagy in cancer cells, thereby stimulating autophagosome formation. In addition, a lysosomotropic agent such as chloroquine (CQ) can result in hyper-accumulation of autophagic vacuoles by inhibiting autophagosome-lysosome fusion, which can drive the cell towards apoptosis. Hence, we postulated that combination treatment with SAHA and CQ may lead to increased formation of autophagosomes, resulting in its hyper-accumulation and ultimately inducing cell death in GBM cells. In the present study, we demonstrated that CQ co-treatment enhanced SAHA-mediated GBM cell apoptosis. Inhibition of the early stage of autophagy by 3-methyladenine pre-treatment reduced cell death confirming that apoptosis induced by CQ and SAHA was dependent on autophagosome accumulation. We also demonstrated that autophagy inhibition led to enhanced ROS, mitochondria accumulation and reduced mitochondrial membrane potential resulting in cell death. The present study provides cellular and molecular evidence concerning the combined effect of SAHA and CQ which can be developed as a therapeutic strategy for the treatment of glioblastoma in the future.

Correspondence to: Dr Rajdeep Chowdhury, Department of Biological Sciences, Birla Institute of Technology and Science (BITS), Pilani Campus, Pilani, Rajasthan 333031, India
E-mail: rajdeep.chowdhury@pilani.bits-pilani.ac.in

Dr Aniruddha Roy, Department of Pharmacy, Birla Institute of Technology and Science (BITS), Pilani Campus, Pilani, Rajasthan 333031, India
E-mail: aniruddha.roy@pilani.bits-pilani.ac.in

Abbreviations: SAHA, suberanilohydroxamic acid; GBM, glioblastoma multiforme; TMZ, temozolomide; CQ, chloroquine; ROS, reactive oxygen species; MMP, mitochondrial membrane potential; MDC, monodansylcadaverine; LC3B-II, microtubule-associated protein light chain 3-II

Key words: glioblastoma multiforme, temozolomide, SAHA, chloroquine

Introduction

Glioblastoma multiforme (GBM), which is an astrocytic tumor of neuroepithelial tissue, occurs most often in the subcortical white matter of the cerebral hemispheres. Tumor infiltration often extends into the adjacent cortex of the basal ganglia and becomes substantially large before turning symptomatic (1). A growing tumor causes an increase of intracranial pressure and sometimes it leads to hydrocephaly (2). GBM is also characterized by high proliferative activity, a large network of hyperplastic blood vessels and finger-like tentacles which spread out infiltrating other parts of the brain, rendering its complete resection very challenging and radiotherapy inefficient (3,4). Moreover, the blood-brain barrier renders treatment more difficult and tumor cells found in hypoxic areas become resistant (5,6). Surgical resection, followed by chemotherapy and radiotherapy is the mainstay of GBM treatment. However, it offers only limited survival advantages (7). Gliomas have been divided into grades I-IV on the basis of the degree of malignancy by the WHO grading system (8). Grade I gliomas generally behave in a benign manner whereas grades II-IV are malignant and infiltrative to the brain. Among astrocytic gliomas, GBM or grade IV glioma is the most prevalent and aggressive type that poses a unique challenge for treatment due to its predisposition for invasion and proliferation. To complicate the therapeutic scenario these tumors are also highly resistant to conventional therapies (9).

Standard chemotherapy used for GBM involves temozolimide (TMZ). The cytotoxicity of TMZ is thought to result from the formation of O^6-methylguanine in DNA, which

mispairs with thymine during DNA replication triggering futile cycles of the mismatch repair and subsequent DNA damage (10). However, apoptosis occurs only in few of the treated GBM cells and at least 50% of TMZ-treated patients do not respond to it (11). This is thought to be due to the over-expression of O^6-methylguanine methyltransferase (MGMT) and/or lack of a DNA repair pathway in GBM cells (12). In addition, results obtained from studies with intrinsic and acquired TMZ-resistant GBM cells revealed that resistance in GBM is not just mediated by a single molecular event but by multiple ones (13). The overall 5-year survival after radiotherapy with concomitant and adjuvant TMZ treatment is only 9.8% (14). Hence, it is important to explore alternative options for GBM sensitization such as, combining two or more drugs that have different cytotoxic mechanisms or targeting alternate pathways resulting in additive or a synergistic effect.

Indirect evidence from recent studies suggest that autophagy, a cellular homeostatic and recycling mechanism may be highly relevant to gliomas (15). Furthermore, the poor response of GBM to current treatment modalities, which largely depends on apoptosis, makes it all the more important to consider autophagy as an alternative death pathway. Notably, one of the most common genetic alterations observed in GBM are amplification of EGFR or deletion of PTEN resulting in activation of the PI3K/Akt/mTOR pathway promoting survival and drug-resistance (16). However, clinical studies with small molecule inhibitors of EGFR or individual inhibitors of PI3K/mTOR have been disappointing (17,18). A dual inhibitor of PI3K and mTOR has exhibited some promise in gliomas (19). However, therapies targeting components of the RTK/PI3K/Akt/mTOR axis typically promote autophagy, thus playing a cytoprotective role (20). Hence, we assume that combination of autophagy promoters alongside autophagosome-lysosome fusion inhibitors could increase cytotoxicity in GBMs by inducing enhanced autophagic stress. GBM cells with inhibited autophagy may significantly accumulate a higher number of damaged mitochondria (due to its reduced clearance by mitophagy) and protein aggregates which can lead to elevated levels of ROS resulting in enhanced cell death. In corroboration to the aforementioned, combination of bafilomycin (a late-stage autophagy inhibitor) with an mTOR inhibitor was found to enhance glioma cell death (20). However, the outcomes of autophagy inhibition may depend on the cell type, the combination therapy explored and other factors, which are yet to be clearly understood.

Vorinostat (SAHA) is a member of a promising class of antitumor agents, HDACi, that have the capacity to enhance the activity of commonly used autophagy inhibitors in tumor therapy. SAHA is currently being used in the treatment of cutaneous T-cell lymphoma and under clinical trials for multiple other cancer types (21,22). HDACi are most frequently known to induce apoptosis via caspases (23), however, more recently, HDACi such as SAHA have been reported to act as inhibitors of the mechanistic target of rapamycin (mTOR) pathway thus increasing autophagy (24). Autophagy activation has been frequently demonstrated to inhibit the onset of apoptotic cell death, however, in certain cases autophagy may have an additive role in the death process as well (25). More precisely excessive 'self-eating' through autophagy or accumulation of autophagosomes may contribute to cell death. In this context, lysosomotropic agents such as chloroquine (CQ) are known to increase the lysosomal pH, which leads to inhibition of the fusion of the autophagosome with the lysosome, resulting in hyper-accumulation of autophagic vacuoles which expedite apoptotic cell death (26). Hence, we presumed that a combination treatment of SAHA and CQ may lead to increased formation of autophagosomes and suppression of the autophagosome-lysome fusion, resulting in hyper-accumulation of autophagic vacuoles, ultimately leading to the enhanced death of GBM cells. Collectively, combining SAHA therapy with autophagy inhibition can be a promising clinical approach in GBM treatment.

Materials and methods

Chemicals and reagents. 2',7'-Dichlorofluorescin diacetate (DCFDA; cat. no. D6883), monodansylcadaverine (MDC; cat. no. D4008), chloroquine-di-phosphate (CQ; cat. no. C6528), propidium iodide (PI; cat. no. P4864) were all purchased from Sigma-Aldrich (St. Louis, MO, USA). N-Acetyl-L-cysteine (NAC; cat. no. 47866) and 3-(4,5-dimethylthiazol-2-yl)-2,5-diphenyltetrazolium bromide (MTT; cat. no. 33611) were obtained from Sisco Research Laboratories Pvt. Ltd. (SRL; Mumbai, India). FITC-conjugated Annexin V (cat. no. A13199) and Annexin V binding buffer (cat. no. V13246), MitoTracker Deep Red FM (cat. no. M22426) and LysoTracker Green DND-26 (cat. no. L7526) were procured from Thermo Fisher Scientific, Inc. (Waltham, MA, USA). JC-1 (cat. no. sc-364116A) was purchased from Santa Cruz Biotechnology (Dallas, TX, USA).

Cell culture. The U87MG cell line was obtained from The National Centre for Cell Science (NCCS; Pune, India) and cultured at 37˚C and 5% CO_2, in Dulbecco's modified Eagle's medium (DMEM) supplemented with 10% fetal bovine serum (FBS; both from Invitrogen; Thermo Fisher Scientific, Inc.; cat. no. 26140-079). Cells were grown to 80% confluency, rinsed in phosphate-buffered saline (PBS) and placed in fresh medium prior to treatment with compounds.

Analysis of cytotoxicity. *In vitro* cytotoxicity was performed following the methods previously described by Chowdhury *et al* (27). Briefly, U87MG cells were seeded at a density of $8x10^4$ cells in 96-well plates. After overnight culture of the cells, they were treated with TMZ, CQ, 3-MA, rapamycin, SAHA, SAHA+CQ for 48 h. Thereafter, MTT was added to each well containing cells and incubated for 4 h. The formazan crystals formed due to the presence of live cells were solubilized in dimethyl sulfoxide (DMSO) and readings were obtained with a spectrophotometer at 570 nm with a differential filter of 630 nm using Multiskan GO microplate spectrophotometer (Thermo Fisher Scientific, Inc.; cat. no. 51119200). The percentage of viable cells was calculated using the formula: Viability (%) = (mean absorbance value of drug-treated cells)/(mean absorbance value of the control) x 100. A concentration of 0.2% DMSO was found to be non-toxic and was used for dissolving SAHA, and used as a control in the cytotoxicity experiments.

Morphological analysis. U87MG cells were seeded at a density of $1x10^6$ cells in 6-well plates and treated with CQ,

SAHA or SAHA+CQ for 48 h. Following the treatment period, images were captured using an Olympus (CKX41) microscope at a x20 magnification (Olympus Corp., Tokyo, Japan).

Apoptosis assay. U87MG cells were seeded at a density of $1x10^6$ cells in a 6-well plate. After overnight culture, the cells were treated with CQ, SAHA, SAHA+CQ for 48 h. Post-treatment, the cells were collected and centrifuged at 380 x g for 5 min at 4˚C. The cell pellet was washed with PBS followed by centrifugation at 380 x g for 5 min at 4˚C. The washed cell pellet was then dissolved in 500 μl of binding buffer. Following this 4 μl of Annexin V/FITC and 10 μl of PI were added. The samples were then incubated in the dark for 20 min and then 10,000 events were acquired in a flow cytometer (CytoFLEX; Beckman Coulter, Brea, CA, USA). The data was analyzed using CytExpert (Beckman Coulter) and the percentage of apoptotic cells was calculated and represented in a bar diagram (27).

Cell cycle analysis. For the analysis of the cells at various phases of the cell cycle, cells were seeded at a density of $1x10^5$, grown overnight and exposed to CQ, SAHA, SAHA+CQ for 48 h. Following incubation with the drugs the cells were collected using PBS, and thereafter fixed in 70% ethanol for 24 h at -20˚C. Following fixation the cell pellet was re-suspended in PBS and then propidium iodide (PI; 20 μg/ml) was added to stain the DNA. The dye-added cell suspension was incubated in the dark for 20 min and then 10,000 events were acquired in a flow cytometer (CytoFLEX; Beckman Coulter). The data was analyzed using CytExpert and the percentage of cells in various phases of the cell cycle was calculated and represented in a bar diagram (27).

Analysis of fragmented DNA using DAPI. U87MG cells were seeded at a density of $1x10^6$, grown overnight and exposed to CQ, SAHA, SAHA+CQ for 48 h. Following treatment for 48 h, the media was removed, the cells were washed with PBS and methanol was added to fix the cells. After 20 min of incubation, a PBS wash was performed to remove the methanol. Then, the cells were stained with DAPI and mounted on slides. The slides were then visualized under a blue filter using a fluorescence microscope (28).

Measurement of intracellular ROS. ROS levels were estimated using DCFHDA (Sigma-Aldrich) which passively enters the cells, where it reacts with ROS to form the highly fluorescent compound, dichlorofluorescein (DCF). U87MG cells were seeded at a density of $8x10^4$ in 96-well plates. After overnight culture of the cells they were treated with CQ, SAHA, SAHA+CQ for 48 h and 5 mM NAC was added 1 h prior to treatment to inhibit ROS. Post-treatment, the cells were washed with PBS and then incubated in 100 μl of working solution of DCFH-DA at 37˚C for 45 min. Following incubation, fluorescence was assessed at a 485 nm excitation and a 530 nm emission using a microplate reader (Fluoroskan Ascent™; cat. no. 5210470; Thermo Fisher Scientific, Inc.) (29).

Measurement of mitochondrial membrane potential. Flow cytometric analysis of mitochondrial membrane potential was performed using the JC-1 dye. U87MG cells were seeded at a density of $1x10^6$ in a 6-well plate. Following overnight culture, the cells were treated with CQ, SAHA, SAHA+CQ for 48 h. Post-treatment, the cells were collected in eppendorf tubes. The cells were centrifuged at 380 x g for 5 min at 4ºC and the total volume was brought to 1 ml using complete DMEM. The cell suspension was stained with 2.5 μg/ml of JC-1 dye. Then, the samples were kept in the dark for 15 min at room temperature (RT). Following this, the cells were centrifuged at 380 x g using double the volume of PBS. Finally, the cells were re-suspended in 300 μl of PBS and analyzed using a flow cytometer (CytoFLEX). The shift from green to red fluorescence was analyzed using CytExpert (27).

Monodansylcadaverine (MDC) staining of autophagic vacuoles. The autofluorescent dye and a specific autophagolysosomal marker, MDC, was used to analyze the autophagic process. U87MG cells were seeded at a density of $1x10^6$ cells in a 6-well plate. Following SAHA+CQ treatment, the cells were incubated for 10 min with 0.05 mM MDC in PBS at 37˚C. Following incubation, the coverslips containing the cells were washed with PBS and mounted with an antifade mountant (containing DAPI). Intracellular MDC in the form of punctate dots were analyzed by fluorescence microscopy. For fluorimetric assessment, following incubation of the cells with CQ, SAHA, SAHA+CQ and labeling with MDC for 10 min, the cells were washed with PBS and collected in 10 mM Tris-HCl (pH 8.0) containing 0.1% Triton X-100. Intracellular MDC was assessed by fluorescence photometry (excitation 380 nm and emission 525 nm) on a microplate reader (Fluoroskan Ascent™) (30,31). An increase in MDC fluorescence upon treatment was expressed as a fold change with respect to the control.

Immunoblotting. U87MG cells were treated with either CQ or SAHA or SAHA plus CQ for 48 h. Thereafter, cells were lysed in a modified RIPA buffer (Sigma-Aldrich; Merck KGaA), and the protein content was measured using the Bradford reagent. Then, the loading buffer was added to the lysates followed by heat denaturation (100˚C for 10 min) and cooling on ice. Equal concentrations of protein lysates were loaded in denaturing polyacrylamide gels and thereafter they were transferred to polyvinylidene fluoride (PVDF) membranes (Thermo Fisher Scientific, Inc.; cat. no. 88518) for blocking with 5% skimmed milk (HiMedia; Mumbai, India; cat. no. GRM1254). The blots were probed with anti-LC3 specific primary antibody at dilution of 1:1,000; (cat. no. 3868; Cell Signaling Technology, Danvers, MA, USA). β-actin (dilution 1:2,000; cat. no. sc69879; Santa Cruz Biotechnology) was used as a loading control. The secondary antibody used was horseradish peroxide-conjugated goat anti rabbit IgG at dilution of 1:10,000 (cat. no. 7074; Cell Signaling Technology). The protein intensity was detected using an enhanced chemiluminescence detection system (Thermo Fisher Scientific, Inc.). The expression levels were densitometrically quantified using ImageJ software (National Institutes of Health, Bethesda, MD, USA) and normalized to the control (27).

Confocal microscopy. U87MG cells were cultured overnight on coverslips and kept in a 35-mm dish at a density of $10x10^6$ cells/dish and then, the cells were exposed to CQ,

SAHA, SAHA+CQ for 48 h. Post-treatment, the media was removed, the cells were washed with PBS, MitoTracker Deep Red was added (MTR, 0.5 μM) and incubation followed for 1 h in humidified air at 37˚C. After incubation, the cells were washed with PBS and methanol was added to fix the cells. Following 20 min of incubation, a PBS wash was performed to remove the methanol. Then, the cells were stained with DAPI and mounted on slides and visualized under a confocal microscope. Excitation of MTR and DAPI at 644 and 358 nm and fluorescence emission was assessed at 665 and 461 nm, respectively (32).

LysoTracker staining of acidic organelles. The LysoTracker Green DND (Thermo Fisher Scientific, Inc.) is a fluorescent probe which is used to visualize acidic organelles in live cells. U87MG cells were cultured overnight on coverslips and kept in a 35-mm dish at a density of $10x10^6$ cells/dish and then cells were exposed to CQ, SAHA, SAHA+CQ for 48 h. Post-treatment, the media was removed, the cells were washed with PBS, LysoTracker Green DND was added (LTG, 0.5 μM) and incubation followed for 20 min in humidified air at 37˚C. Following 20 min of incubation, the cells were stained with DAPI and mounted on slides. The cells were then visualized under a fluorescence microscope and the intensity of LysoTracker fluorescence was compared with the untreated control (32).

Statistical analysis. The obtained data were analyzed using the GraphPrism® software (version 5.01; GraphPad Software, Inc., La Jolla, CA, USA). The effect of various treatments was statistically analyzed using one-way ANOVA and Tukey's multiple comparison test was used for comparison of the control with different tests. All data points represent the mean of independent measurements and were represented as the standard error in the form of bars.

Results

Effect of SAHA and CQ co-treatment on the sensitization of U87MG glioblastoma cells. GBM is one of the deadliest types of brain malignancy with inadequate responsiveness to commonly used therapeutic interventions. Currently, the gold standard treatment for GBM constitutes surgical resection followed by adjuvant chemotherapy with TMZ. However, these tumors have been well documented for their development of resistance to the standard therapy (33). One of the anticipated mechanisms for acquisition of therapeutic resistance in GBM is induction of stress-induced autophagy. However, the precise role of autophagy in cancer development, and its role in response to chemotherapy are highly controversial (9). There are conflicting reports pertaining to TMZ-induced autophagy in GBM. For example, Kanzawa *et al* observed significant autophagy induction following TMZ treatment which acted as a cell death-inducing phenomenon (34); while, subsequent studies have reflected a pro-survival response in GBM cells to TMZ (35). Notably, in most cases, GBM cells when treated with TMZ revealed the onset of apoptosis only after 4-6 days following treatment, where autophagy was an early response inhibitor of cell death (36). The temporal delayed action of TMZ has progressively hindered the use of TMZ in GBM therapy necessitating the search for novel therapy.

In the present study, we first explored the efficacy of HDACi, SAHA for GBM therapy. For this purpose, the human GBM cell line U87MG was selected as the *in vitro* model system since these GBM cells are known to show resistance to TMZ treatment (37). In addition, in the present study we observed that U87MG cells were highly resistant to TMZ as it failed to induce any cytotoxic effect up to a 30-μM concentration and 48 h of exposure (data available upon request). In contrast, these cells were found to be responsive to SAHA treatment. The results revealed that SAHA exhibited dose-dependent cytotoxicity and reduced the cell viability to ~30% with a 30-μM concentration (Fig. 1A). Next, we investigated whether autophagy modulation can increase the cytotoxic effect of SAHA in the U87MG cells. Recent studies have revealed that HDACi, such as SAHA can modulate autophagic protein expression in human cancer cells (38). However, the precise role and the molecular mechanisms underlying HDACi-mediated autophagy are still not clear. Moreover, the role of autophagy in cell death remains controversial and is likely to be context-dependent. We hence determined whether autophagy modulators could lead chemotherapy-resistant GBM cells towards cell death. We studied the activity of different autophagy modulators on the viability of the U87MG cells and found that while early autophagy inhibitor 3-MA did not have any significant effect on cell viability (data available upon request), the lysosomotropic agent- choloroquine (used as the di-phosphate salt, CQ) exhibited dose-dependent cytotoxicity (Fig. 1B). Furthermore, rapamycin, an inhibitor of mTOR signaling, which is often used as an autophagy activator, did not demonstrate any cytotoxic effect (data available upon request). Next, we studied the effect of these autophagy modulators on the SAHA-treated U87MG cells. Notably, co-treatment with SAHA and CQ exhibited significantly higher cytotoxicity (36% viability at 30 μM SAHA and 25 μM CQ) than SAHA or CQ alone, whereas co-treatment with 3-MA or rapamycin along with SAHA had no significant synergistic effect on cytotoxicity (Fig. 1C). Pronounced morphological variations were also observed upon SAHA+CQ combination treatment in the U87MG cells when compared to the control or other treatments (Fig. 1D).

Based on previous studies, it has been established that SAHA induces autophagy (39). In this study, SAHA treatment in U87MG cells exhibited a significant increase in MDC fluorescent punctate dots (Fig. 1E). MDC stains autophagic vacuoles and an increase in MDC fluorescence is often correlated with enhanced autophagy. Additionally, treatment of SAHA+CQ revealed a 3-fold increase in MDC fluorescence in comparison to only SAHA, as analyzed by fluorimetry (Fig. 1F). Chloroquine is known to act by increasing lysosomal pH and thereby inhibiting lysosomal activity (40). MDC on the other hand is known to label not only acidic lysosomes but also endosomes and autophagosomes (41); i.e., MDC can incorporate into membranes based on lipid characteristics independent of pH (42). Since, CQ increases the accumulation of autophagosomes or autophagic vacuoles, we observed an increased MDC fluorescence in CQ-treated cells that increased even further upon treatment with SAHA plus CQ. This was likely to be the MDC trapped in the accumulated vacuoles after CQ treatment. Furthermore, the increased MDC fluorescence with SAHA+CQ treatment could

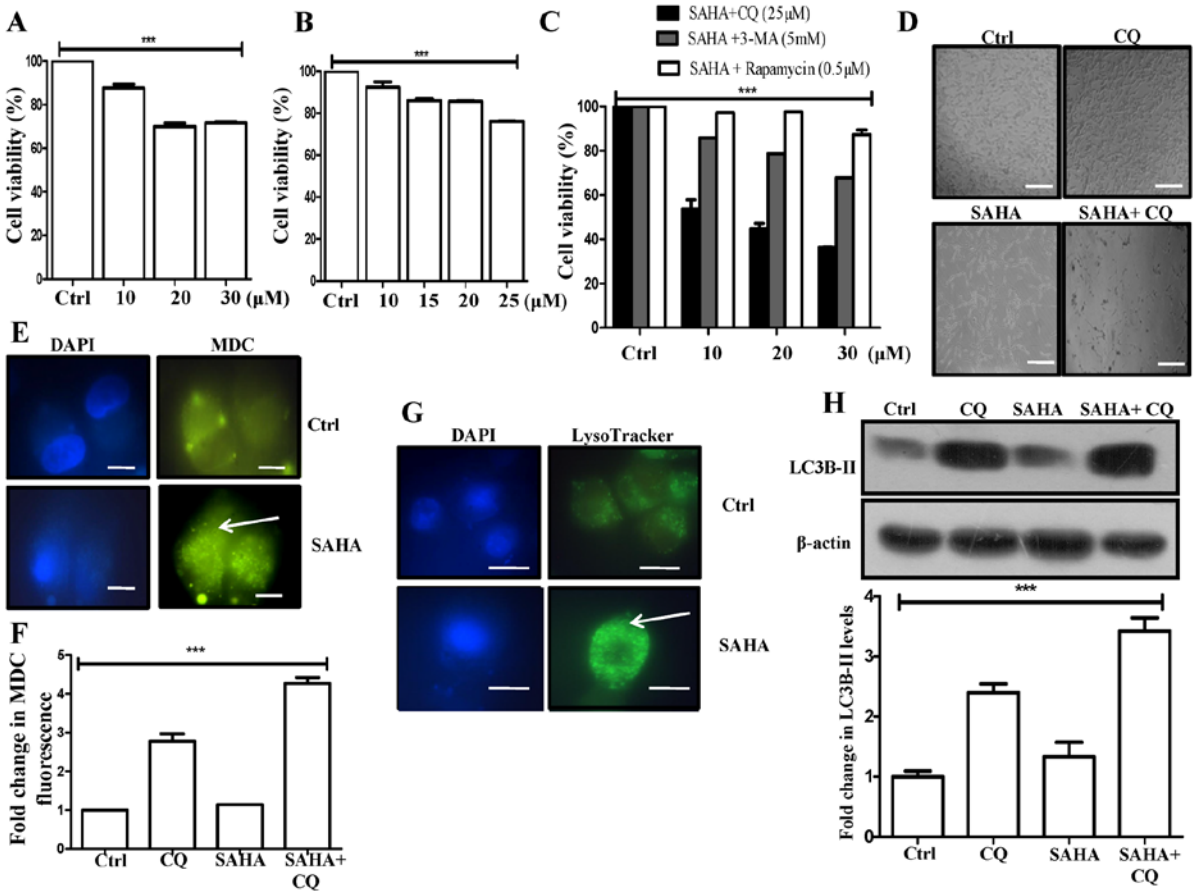

Figure 1. SAHA and CQ co-treatment leads to higher cell death through autophagosome accumulation. (A) Cells were treated with SAHA for 48 h, and the cell viability was analyzed using an MTT assay. The symbol *** represents a significant difference (P<0.05) as compared to the untreated control cells. (B) The effect of CQ treatment at different concentrations on the U87MG cell line for 48 h. The symbol *** represents a significant difference (P<0.05) as compared to the untreated control cells. (C) Effect of SAHA in combination with CQ or 3-MA or rapamycin in the U87MG cell line for 48 h. The symbol *** represents a significant difference (P<0.05) as compared to the untreated cells. (D) Bright field images of the U87MG cell line post-treatment with CQ, SAHA, SAHA+CQ for 48 h. Scale bar, 100 μm. (E) MDC fluorescence staining was performed after 48 h of SAHA treatment at a 20-μM dose in the U87MG cells and green punctate dots indicative of autophagosomes were monitored by fluorescence microscopy. The scale bar represents 100 μm. (F) Fluorimetric estimation of MDC activity was performed following SAHA+CQ treatment for 48 h in the U87MG cells. The symbol *** represents a significant difference (P<0.05) as compared to the untreated cells. (G) Cells were treated with SAHA at 20 μM for 48 h and then stained with LysoTracker; green dots representing lysosomes were monitored by fluorescence microscopy. (H) Protein expression of autophagy marker, LC3B-II was studied by immunoblotting after SAHA (20μM) + CQ (25 μM) treatment. Densitometric analysis of the scanned immunoblot was performed by ImageJ software. β-actin was served as a loading control. The symbol *** represents a significant difference (P<0.05) as compared to untreated cells.

be attributed to the fact that SAHA induces autophagy while CQ blocks autophagic flux resulting in increased accumulation of autophagic vacuoles leading to even more trapping of MDC in them. Hence, MDC fluorescence was the highest in the combination treatment, followed by treatment only with CQ, and then SAHA-treated samples.

On a similar note, SAHA treatment also increased green punctate dots with stronger fluorescence intensity indicating an enhanced lysosomal number in comparison to the control, as analyzed through LysoTracker staining, in GBM cells (Fig. 1G). This is supportive of the view that SAHA triggers autophagy in U87MG cells. In addition, microtubule-associated protein light chain 3-II (LC3B-II), an autophagic marker, exhibited a significant increase in the SAHA+CQ combination treatment, than only the CQ treatment reflecting the induction of autophagic flux by administration of SAHA (Fig. 1H). We assumed that inhibition of autophagosome-lysosome fusion by CQ presumably resulted in an increased autophagosome accumulation evident from enhanced MDC fluorescence in the combination treatment (Fig. 1F). Our results revealed that blocking of SAHA-induced autophagy by inhibitors of autophagic flux can increase SAHA-mediated cell death preferentially in U87MG cells. However, upstream autophagic block or autophagy inducers have limited effect on cell death.

Inhibition of autophagy by CQ potentiates SAHA-mediated apoptosis. We were thereafter interested in understanding the mode of cell death by the combination treatment. According to present literature, the primary antitumor activity of HDACi is believed to be through induction of apoptosis in a variety of cancer cells (43). Moreover, recent studies have also demonstrated that HDACi, such as SAHA can also induce autophagy in human cancer cells (39). However, currently the role of HDACi-mediated autophagy in context to apoptosis remains controversial and is still not clear. We hence analyzed apoptosis using Annexin V-FITC/PI dye with SAHA and CQ treatment using flow cytometry. The Annexin V-FITC conjugate binds to phosphotidyl serine on the cell surface

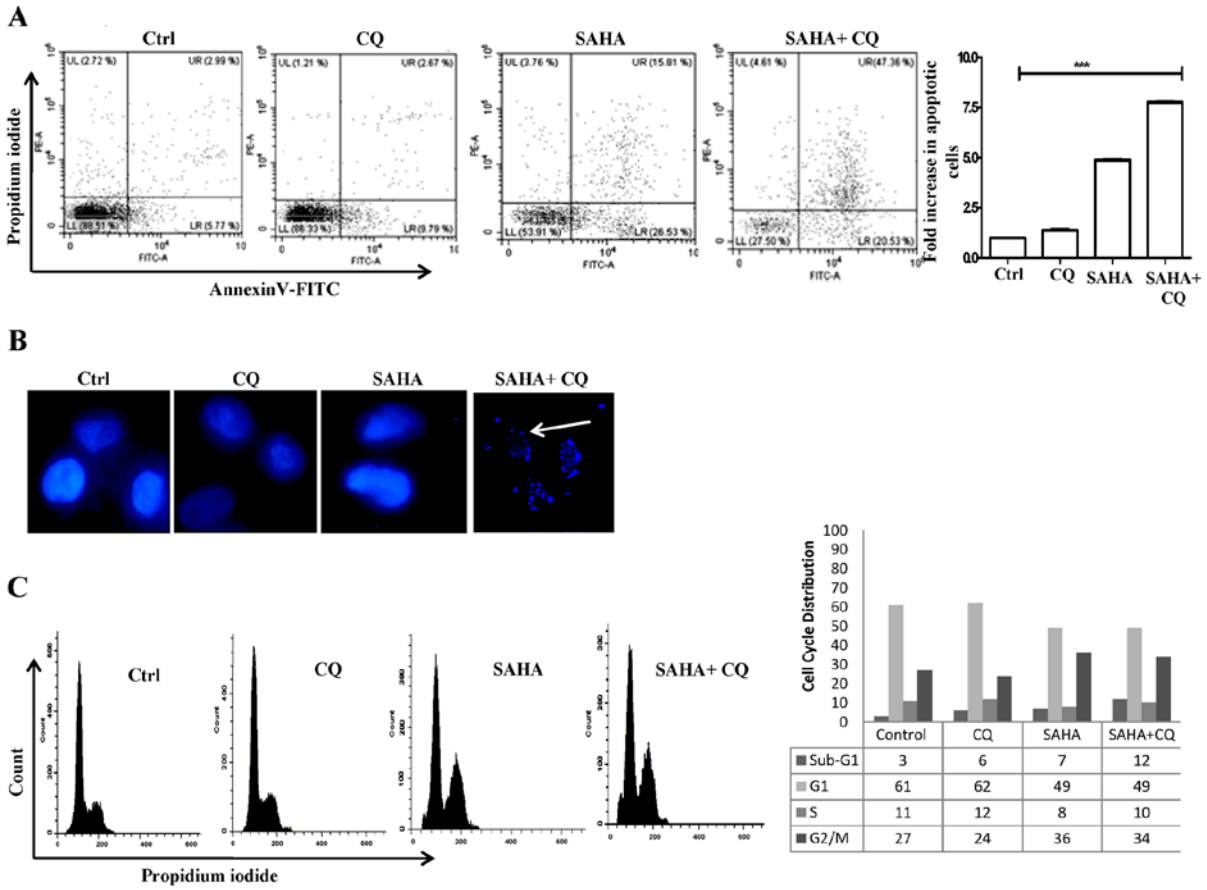

	Control	CQ	SAHA	SAHA+CQ
Sub-G1	3	6	7	12
G1	61	62	49	49
S	11	12	8	10
G2/M	27	24	36	34

Figure 2. SAHA and CQ co-treatment induces apoptosis. (A) Assessment of apoptosis using flow cytometry, post 48 h of SAHA (20 μM) and/or CQ treatment. In the representative images, cells in the lower right (LR) and upper right (UR) quadrant represent early and late apoptosis, respectively. Fold increase in the early and late apoptotic cells was combined and calculated with respect to the untreated control (taken as arbitrary unit 1), which is represented by a bar diagram. The symbol *** represents a significant difference (P<0.05) as compared to the untreated control cells. (B) DAPI staining revealing the fragmented nucleus upon exposure of cells to CQ (25 μM) or SAHA (20 μM) or SAHA and CQ. (Scale bar, 50 μm). (C) Cell cycle analysis using PI staining revealing an increase in the subG$_1$ population of cells post SAHA (20 μM) and/or CQ (25 μM) treatment for 48 h. A representative image of flow cytometric analysis is provided. Percentage of cells in each phase of the cell cycle- sub-G$_1$, G$_1$, S and G$_2$/M is depicted.

and detects cells in the early stages of apoptosis and PI binds to fragmented DNA and detects cells that have undergone cell death, while cells positive for both represents late apoptosis. Upon treatment with only SAHA, a significant percentage (42.34%; 4.83-fold) of cells were found to undergo apoptosis when compared to the control (Fig. 2A). This was expected, since SAHA is known to induce apoptosis. Only CQ treatment failed to exhibit any significant increase in apoptotic cells. However, cells treated with SAHA+CQ exhibited a marked increase (67.89%; 7.74-fold to the control) in apoptotic cells (Fig. 2A). This is indicative of the fact that inhibition of autophagic flux increases SAHA-induced apoptosis. To confirm cell death, DAPI staining of the nucleus was also performed to check for fragmented DNA, as DNA fragmentation is a hallmark of apoptosis. The presence of fragmented nuclei, indicative of the apoptotic process, in the SAHA+CQ-treated cells is shown in Fig. 2B. We thereafter examined the effect of the combination treatment on the cell cycle. SAHA treatment increased the cell population at the G$_2$/M phase whereas, with the combination treatment, there was a significant increase in the sub G1 population of cells from 7 to 12%, which confirmed the induction of apoptosis (Fig. 2C). These data revealed that simultaneous induction of autophagosome formation and inhibition of autophagosome-lysosomal fusion in U87MG cells by SAHA+CQ treatment was associated with increased apoptotic cell death compared to only HDACi treatment.

SAHA+CQ increases ROS production leading to enhanced apoptosis in GBM cells. Autophagy can potentially act as a pro-survival strategy in response to drug stress by eliminating damaged intra-cellular mitochondria by a process known as mitophagy (44). In normal conditions, ROS generated during mitochondrial oxidative metabolism plays an important role in the maintenance of cellular homeostasis. However, cancer cells due to extensive proliferative requirements tend to generate excess ROS than normal cells. In addition, they utilize intricate cellular mechanisms to keep a check on ROS levels which if not can be fatal for the tumor cells. Under stress, cancer cells can also limit ROS accumulation via an increase in cytoprotective selective autophagy e.g., mitophagy to facilitate higher proliferation, metastasis and also resistance against drug treatment (45). As aforementioned, we observed that SAHA induces autophagy and when autophagy is inhibited by CQ autophagosomes presumably accumulate, as observed through increased MDC fluorescence in the combination treatment. We found that co-treatment with SAHA and CQ resulted in

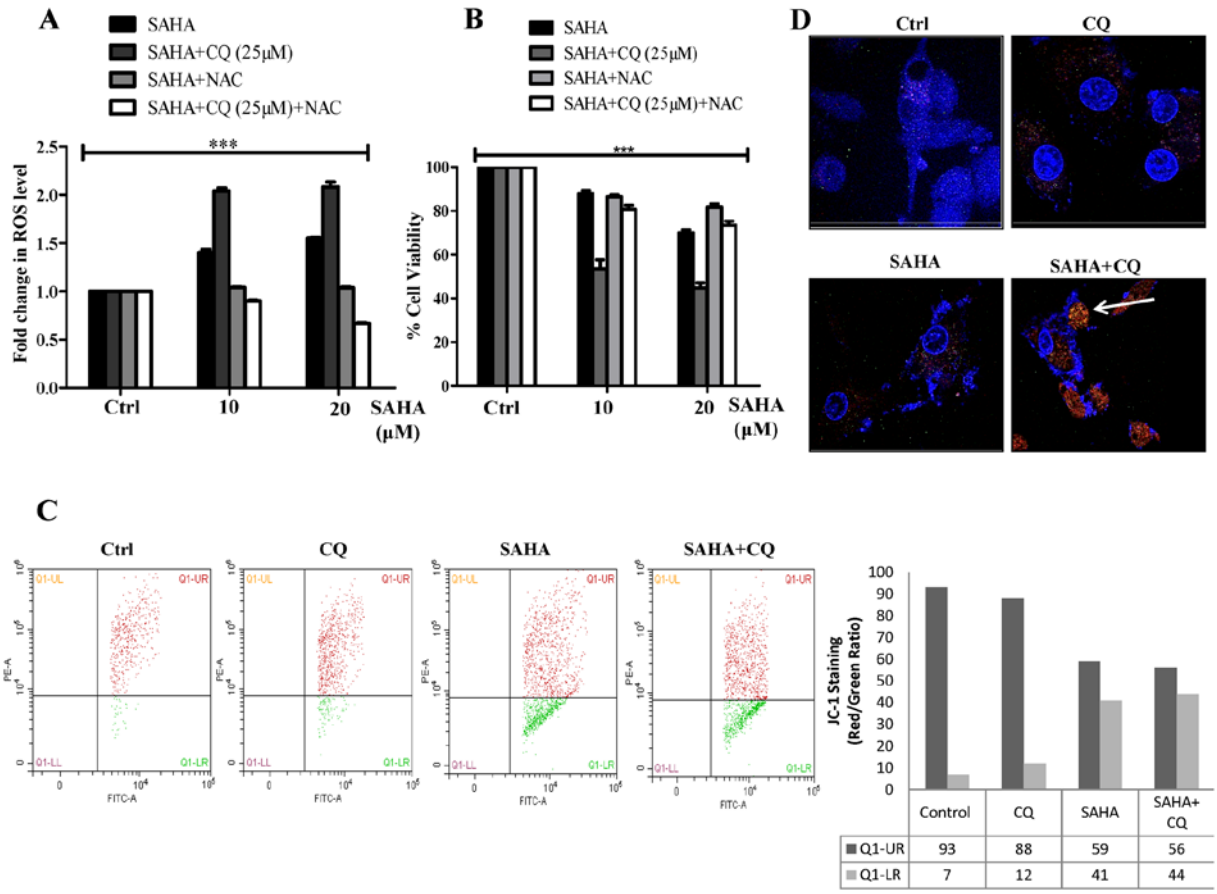

Figure 3. SAHA and CQ co-treatment results in increased ROS formation. (A) H_2DCFDA fluorimetric assay estimating ROS upon SAHA and/or CQ exposure at different concentrations for 48 h. NAC (5 mM) was applied 1 h prior to treatment wherever mentioned. Fold change in ROS levels is represented; the untreated control was considered as arbitrary unit '1'. The symbol *** represents a significant difference (P<0.05) as compared to the untreated control cells. (B) Measurement of cell viability by MTT assay upon addition of ROS quencher NAC (5 mM), applied 1 h prior to treatment, in SAHA- and/or CQ-exposed cells. The symbol *** represents a significant difference (P<0.05) as compared to the untreated control cells. (C) JC-1 assay was performed using flow cytometry, revealing a shift from red to green fluorescence indicative of a change in mitochondrial membrane potential. (D) MitoTracker Red staining was performed in U87MG cells after treatment with SAHA and/or CQ for 48 h. Red dots indicative of mitochondria were monitored by confocal microscopy.

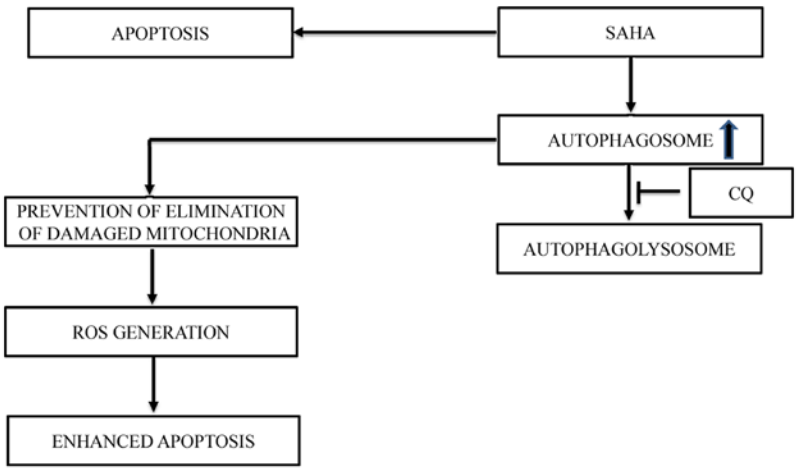

Figure 4. Schematic representation of the probable mechanism involved in SAHA and CQ-induced cell death. SAHA is known to induce apoptosis as well as to increase autophagosome formation. However, the autophagosome would be cleared from the cell by fusion with a lysosome. Conversely, when CQ is co-treated with SAHA, CQ inhibits the clearance of the autophagosome by inhibiting the phago-lysosomal fusion. This leads to an increased accumulation of phagosomes in the cells. Damaged mitochondria also accumulate which leads to increased ROS generation. All these result in enhanced apoptosis in the treated cells.

a significant increase in ROS production, maybe due to the inhibition of autophagic flux (Fig. 3A). SAHA has been previously demonstrated to simultaneously induce apoptosis by increasing ROS production and also trigger autophagy (39,46). Autophagy under this circumstance, presumably acts as a survival strategy by clearance of damaged mitochondria

generated by SAHA treatment, thus maintaining cellular homeostasis and survival. However, with the addition of CQ along with SAHA, selective autophagy is inhibited leading to excess ROS accumulation. Notably, when ROS was quenched in the SAHA+CQ-treated cells by the ROS scavenger (*N*-acetyl cysteine, NAC), cell viability increased (Fig. 3B) which confirmed that SAHA+CQ-mediated enhanced cell death was significantly dependent on ROS. The accumulation of ROS with the combination treatment was also associated with mitochondrial membrane potential (MMP) reduction, a prerequisite to cell death. Upon treatment with SAHA+CQ, not only did the amount of ROS increase but it also led to increased collapse of MMP as determined by JC-1 assay (Fig. 3C). To further validate the hypothesis that CQ induces mitochondria accumulation in SAHA-treated cells, we used confocal microscopy with MitoTracker Red dye. The results revealed MitoTracker Red indicative of the number of mitochondria significantly accumulated in the SAHA-treated cells in which autophagic flux was blocked with CQ (Fig. 3D). The aforementioned result along with increased ROS confirm that damaged mitochondria accumulated in the SAHA+CQ-treated cells lead to increased apoptosis.

Discussion

For decades temozolomide (TMZ), has been the drug of choice for glioblastoma multiforme (GBM) (47). Yet, a major hindrance to TMZ therapy has been the intrinsic or acquired resistance of GBM patients (48). Recent studies also revealed that TMZ could induce autophagy in GBM cells. However, TMZ-induced autophagy also induced a cytoprotective ATP surge in glioma cells (49,50). Furthermore, in contrast to the aforementioned, a recent study also reported that rapamycin, an autophagy activator could enhance glioma cell sensitization *in vitro* and in immuno-compromised mice (51). These findings along with reports of acquired resistance of GBM cells necessitate the design of alternate therapeutic strategies for effective treatment of GBM. Similarly, the role of autophagy in GBM is also not clearly understood as conflicting observations portray both its cytoprotective as well as pro-apoptotic role.

Recent studies indicate that HDACi such as SAHA, in addition to their ability to induce apoptosis are also capable of stimulating autophagy. SAHA has a wide range of effects extending from inhibition of cell cycle progression, suppression of the angiogenic effect to the induction of apoptosis in cancer cells (52). However, in addition to its role in apoptosis SAHA has also been reported to promote autophagic cell death, which offers an obvious advantage for therapy against apoptosis-resistant tumor cells (53,54). We therefore explored SAHA as a therapeutic agent in combination with known autophagy modulators. Anti-malarial drugs such as choloroquine that block autophagic flux by inhibiting lysosomal acidification, are currently in clinical trials in combination with TMZ for treatment of GBM (55). While we are still awaiting the results from these trials, we wondered about the consequences of simultaneous application of SAHA and CQ in GBM cells. We also tried increasing the autophagy levels with mTOR inhibitor, rapamycin, alongside SAHA, realizing that an enhanced autophagy would lead GBM cells from proliferation towards cell death. Notably, while the use of rapamycin along with SAHA had a limited effect on the survival of GBM cells, concurrent treatment of SAHA+CQ resulted in significant cell death. Moreover, inhibition of upstream autophagy events with 3-MA also had a reduced effect on SAHA-induced cytotoxicity in GBM cells suggesting that modulation of autophagic flux has an enhanced effect than the inhibition of the early steps of autophagy.

There is an increasing body of evidence suggesting that in cancer cells, the autophagy-lysosomal pathway integrates signals from varied upstream events thereby resulting in an intricate regulatory mechanism which can culminate in cell death or survival (56,57). However, the roadmap to the ultimate effect in a particular cancer cell is purely context-dependent and this knowledge is critical for formulating effective therapeutic strategies (58-60). Hence, this becomes increasingly important in the context of glioma cells, which display significant therapeutic resistance against conventionally used drugs. In the present study, we revealed that the combination treatment of SAHA and CQ resulted in an increase of damaged mitochondria accumulation in U87MG cells leading to a significant increase in ROS levels and a reduction in mitochondrial membrane potential, triggering apoptosis. We postulated that the lack of clearance of damaged mitochondria by mitophagy in these cells post-treatment with SAHA and CQ could be the cause of the induction of cell death (Fig. 4). We further revealed that inhibition of autophagy at a late stage, but not at an early stage, increased the cytotoxic effect of SAHA via apoptosis. Hence, this study provides cellular and molecular evidence concerning the combined effect of SAHA and CQ which can be developed as a therapeutic strategy for glioblastoma treatment in future.

Acknowledgements

We acknowledge BITS-Pilani for providing us with infrastructural support. LK would like to thank BITS-Pilani for providing support for his master's thesis.

Funding

The present study was supported in part by the DST-SERB grant of SM (SERB/LS-77/2013), RC (SB/FT/LS-233/2012) and the DBT grant of RC (BT/PR/8799/MED/30/1067/2013).

Availability of data and materials

The datasets used during the present study are available from the corresponding author upon reasonable request.

Authors' contributions

LK, HS, AS and SM performed and analyzed the experiments. RC and AR designed and planned the study; RC, AR and LK wrote the manuscript. All authors read and approved the manuscript and agree to be accountable for all aspects of the research in ensuring that the accuracy or integrity of any part of the work are appropriately investigated and resolved.

Ethics approval and consent to participate

Not applicable.

Consent for publication

Not applicable.

Competing interests

The authors declare that they have no competing interests.

References

1. Iacob G and Dinca EB: Current data and strategy in glioblastoma multiforme. J Med Life 2: 386-293, 2009.
2. Jung WH, Choi S, Oh KK and Chi JG: Congenital glioblastoma multiforme-report of an autopsy case. J Korean Med Sci 5: 225-231, 1990.
3. Wang R, Chadalavada K, Wilshire J, Kowalik U, Hovinga KE, Geber A, Fligelman B, Leversha M, Brennan C and Tabar V: Glioblastoma stem-like cells give rise to tumour endothelium. Nature 468: 829-833, 2010.
4. Linkous AG and Yazlovitskaya EM: Angiogenesis in glioblastoma multiforme: Navigating the maze. Anticancer Agents Med Chem 11: 712-718, 2011.
5. Van Tellingen O, Yetkin-Arik B, de Gooijer MC, Wesseling P, Wurdinger T and de Vries HE: Overcoming the blood-brain tumor barrier for effective glioblastoma treatment. Drug Resist Updat 19: 1-12, 2015.
6. Huang WJ, Chen WW and Zhang X: Glioblastoma multiforme: Effect of hypoxia and hypoxia inducible factors on therapeutic approaches. Oncol Lett 12: 2283-2288, 2016.
7. Thomas AA, Ernstoff MS and Fadul CE: Immunotherapy for the treatment of glioblastoma. Cancer J 18: 59-68, 2012.
8. Jovčevska I, Kočevar N and Komel R: Glioma and glioblastoma-how much do we (not) know? Mol Clin Oncol 1: 935-941, 2013.
9. Sui X, Chen R, Wang Z, Huang Z, Kong N, Zhang M, Han W, Lou F, Yang J, Zhang Q, *et al*: Autophagy and chemotherapy resistance: A promising therapeutic target for cancer treatment. Cell Death Dis 4: e838, 2013.
10. Zhang J, Stevens MF and Bradshaw TD: Temozolomide: Mechanisms of action, repair and resistance. Curr Mol Pharmacol 5: 102-114, 2012.
11. Beier D, Schulz JB and Beier CP: Chemoresistance of glioblastoma cancer stem cells-much more complex than expected. Mol Cancer 10: 128, 2011.
12. Wilson TA, Karajannis MA and Harter DH: Glioblastoma multiforme: State of the art and future therapeutics. Surg Neurol Int 5: 64, 2014.
13. Haar CP, Hebbar P, Wallace GC IV, Das A, Vandergrift WA III, Smith JA, Giglio P, Patel SJ, Ray SK and Banik NL: Drug resistance in glioblastoma: A mini review. Neurochem Res 37: 1192-1200, 2012.
14. Stupp R, Hegi ME, Mason WP, van den Bent MJ, Taphoorn MJ, Janzer RC, Ludwin SK, Allgeier A, Fisher B, Belanger K, *et al*: Effects of radiotherapy with concomitant and adjuvant temozolomide versus radiotherapy alone on survival in glioblastoma in a randomised phase III study: 5-year analysis of the EORTC-NCIC trial. Lancet Oncol 10: 459-466, 2009.
15. Kaza N, Kohli L and Roth KA: Autophagy in brain tumors: A new target for therapeutic intervention. Brain Pathol 22: 89-98, 2012.
16. Cheng CK, Fan QW and Weiss WA: PI3K signaling in glioma-animal models and therapeutic challenges. Brain Pathol 19: 112-120, 2009.
17. Carrasco-García E, Saceda M, Grasso S, Rocamora-Reverte L, Conde M, Gómez-Martínez A, García-Morales P, Ferragut JA and Martínez-Lacaci I: Small tyrosine kinase inhibitors interrupt EGFR signaling by interacting with erbB3 and erbB4 in glioblastoma cell lines. Exp Cell Res 317: 1476-1489, 2011.
18. Rich JN, Reardon DA, Peery T, Dowell JM, Quinn JA, Penne KL, Wikstrand CJ, Van Duyn LB, Dancey JE, McLendon RE, *et al*: Phase II trial of gefitinib in recurrent glioblastoma. J Clin Oncol 22: 133-142, 2004.
19. Fan QW, Knight ZA, Goldenberg DD, Yu W, Mostov KE, Stokoe D, Shokat KM and Weiss WA: A dual PI3 kinase/mTOR inhibitor reveals emergent efficacy in glioma. Cancer Cell 9: 341-349, 2006.
20. Fan QW, Cheng C, Hackett C, Feldman M, Houseman BT, Nicolaides T, Haas-Kogan D, James CD, Oakes SA, Debnath J, *et al*: Akt and autophagy cooperate to promote survival of drug-resistant glioma. Sci Signal 3: ra81, 2010.
21. Duvic M, Talpur R, Ni X, Zhang C, Hazarika P, Kelly C, Chiao JH, Reilly JF, Ricker JL, Richon VM and Frankel SR: Phase 2 trial of oral vorinostat (suberoylanilide hydroxamic acid, SAHA) for refractory cutaneous T-cell lymphoma (CTCL). Blood 109: 31-39, 2007.
22. Munster PN, Thurn KT, Thomas S, Raha P, Lacevic M, Miller A, Melisko M, Ismail-Khan R, Rugo H, Moasser M and Minton SE: A phase II study of the histone deacetylase inhibitor vorinostat combined with tamoxifen for the treatment of patients with hormone therapy-resistant breast cancer. Br J Cancer 104: 1828-1835, 2011.
23. Shao Y, Gao Z, Marks PA and Jiang X: Apoptotic and autophagic cell death induced by histone deacetylase inhibitors. Proc Natl Acad Sci USA 101: 18030-18035, 2004.
24. Hrzenjak A, Kremser ML, Strohmeier B, Moinfar F, Zatloukal K and Denk H: SAHA induces caspase-independent, autophagic cell death of endometrial stromal sarcoma cells by influencing the mTOR pathway. J Pathol 216: 495-504, 2008.
25. Yonekawa T and Thorburn A: Autophagy and cell death. Essays Biochem 55: 105-117, 2013.
26. Kim EL, Wüstenberg R, Rübsam A, Schmitz-Salue C, Warnecke G, Bücker EM, Pettkus N, Speidel D, Rohde V, Schulz-Schaeffer W, *et al*: Chloroquine activates the p53 pathway and induces apoptosis in human glioma cells. Neuro Oncol 12: 389-400, 2010.
27. Chowdhury R, Chowdhury S, Roychoudhury P, Mandal C and Chaudhuri K: Arsenic induced apoptosis in malignant melanoma cells is enhanced by menadione through ROS generation, p38 signaling and p53 activation. Apoptosis 14: 108-123, 2009.
28. Pajaniradje S, Mohankumar K, Pamidimukkala R, Subramanian S and Rajagopalan R: Antiproliferative and apoptotic effects of *Sesbania grandiflora* leaves in human cancer cells. Biomed Res Int 2014: 474953, 2014.
29. Laporte AN, Barrott JJ, Yao RJ, Poulin NM, Brodin BA, Jones KB, Underhill TM and Nielsen TO: HDAC and proteasome inhibitors synergize to activate pro-apoptotic factors in synovial sarcoma. PLoS One 12: e0169407, 2017.
30. Mizushima N: Methods for monitoring autophagy. Int J Biochem Cell Biol 36: 2491-2502, 2004.
31. Munafó DB and Colombo MI: A novel assay to study autophagy: Regulation of autophagosome vacuole size by amino acid deprivation. J Cell Sci 114: 3619-3629, 2001.
32. Rodriguez-Enriquez S, Kim I, Currin RT and Lemasters JJ: Tracker dyes to probe mitochondrial autophagy (mitophagy) in rat hepatocytes. Autophagy 2: 39-46, 2006.
33. Adamson C, Kanu OO, Mehta AI, Di C, Lin N, Mattox AK and Bigner DD: Glioblastoma multiforme: A review of where we have been and where we are going. Expert Opin Investig Drugs 18: 1061-1083, 2009.
34. Kanzawa T, Bedwell J, Kondo Y, Kondo S and Germano IM: Inhibition of DNA repair for sensitizing resistant glioma cells to temozolomide. J Neurosurg 99: 1047-1052, 2003.
35. Fu J, Liu ZG, Liu XM, Chen FR, Shi HL, Pangjesse CS, Ng HK and Chen ZP: Glioblastoma stem cells resistant to temozolomide-induced autophagy. Chin Med J (Engl) 122: 1255-1259, 2009.
36. Wojton J, Elder J and Kaur B: How efficient are autophagy inhibitors as treatment for glioblastoma? CNS Oncol 3: 5-7, 2014.
37. Hegi ME, Liu L, Herman JG, Stupp R, Wick W, Weller M, Mehta MP and Gilbert MR: Correlation of O6-methylguanine methyltransferase (MGMT) promoter methylation with clinical outcomes in glioblastoma and clinical strategies to modulate MGMT activity. J Clin Oncol 26: 4189-4199, 2008.
38. Liu YL, Yang PM, Shun CT, Wu MS, Weng JR and Chen CC: Autophagy potentiates the anti-cancer effects of the histone deacetylase inhibitors in hepatocellular carcinoma. Autophagy 6: 1057-1065, 2010.
39. Gammoh N, Lam D, Puente C, Ganley I, Marks PA and Jiang X: Role of autophagy in histone deacetylase inhibitor-induced apoptotic and nonapoptotic cell death. Proc Natl Acad Sci USA 109: 6561-6565, 2012.
40. Guha S, Coffey EE, Lu W, Lim JC, Beckel JM, Laties AM, Boesze-Battaglia K and Mitchell CH: Approaches for detecting lysosomal alkalinization and impaired degradation in fresh and cultured RPE cells: Evidence for a role in retinal degenerations. Exp Eye Res 126: 68-76, 2014.

41. Perry CN, Kyoi S, Hariharan N, Takagi H, Sadoshima J and Gottlieb RA: Novel methods for measuring cardiac autophagy in vivo. Methods Enzymol 453: 325-342, 2009.
42. Iwai-Kanai E, Yuan H, Huang C, Sayen MR, Perry-Garza CN, Kim L and Gottlieb RA: A method to measure cardiac autophagic flux in vivo. Autophagy 4: 322-329, 2008.
43. Kim HJ and Bae SC: Histone deacetylase inhibitors: molecular mechanisms of action and clinical trials as anti-cancer drugs. Am J Transl Res 3: 166-179, 2011.
44. Gomes LR, Vessoni AT and Menck CFM: Microenvironment and autophagy cross-talk: Implications in cancer therapy. Pharmacol Res 107: 300-307, 2016.
45. Poillet-Perez L, Despouy G, Delage-Mourroux R and Boyer-Guittaut M: Interplay between ROS and autophagy in cancer cells, from tumor initiation to cancer therapy. Redox Biol 4: 184-192, 2015.
46. Ruefli AA, Ausserlechner MJ, Bernhard D, Sutton VR, Tainton KM, Kofler R, Smyth MJ and Johnstone RW: The histone deacetylase inhibitor and chemotherapeutic agent suberoylanilide hydroxamic acid (SAHA) induces a cell-death pathway characterized by cleavage of Bid and production of reactive oxygen species. Proc Natl Acad Sci USA 98: 10833-10838, 2001.
47. Ray S, Bonafede MM and Mohile NA: Treatment patterns, survival, and healthcare costs of patients with malignant gliomas in a large US commercially insured population. Am Health Drug Benefits 7: 140-149, 2014.
48. Zhang J, Stevens MF, Laughton CA, Madhusudan S and Bradshaw TD: Acquired resistance to temozolomide in glioma cell lines: Molecular mechanisms and potential translational applications. Oncology 78: 103-114, 2010.
49. Fulda S and Kögel D: Cell death by autophagy: Emerging molecular mechanisms and implications for cancer therapy. Oncogene 34: 5105-5113, 2015.
50. Katayama M, Kawaguchi T, Berger M and Pieper R: DNA damaging agent-induced autophagy produces a cytoprotective adenosine triphosphate surge in malignant glioma cells. Cell Death Differ 14: 548-558, 2007.
51. Voss V, Senft C, Lang V, Ronellenfitsch MW, Steinbach JP, Seifert V and Kögel D: The pan-Bcl-2 inhibitor (-)-gossypol triggers autophagic cell death in malignant glioma. Mol Cancer Res 8: 1002-1016, 2010.
52. Falkenberg KJ and Johnstone RW: Histone deacetylases and their inhibitors in cancer, neurological diseases and immune disorders. Nat Rev Drug Discov 13: 673-691, 2014.
53. Lee YJ, Won AJ, Lee J, Jung JH, Yoon S, Lee BM and Kim HS: Molecular mechanism of SAHA on regulation of autophagic cell death in tamoxifen-resistant MCF-7 breast cancer cells. Int J Med Sci 9: 881-993, 2012.
54. Carew JS, Nawrocki ST, Kahue CN, Zhang H, Yang C, Chung L, Houghton JA, Huang P, Giles FJ and Cleveland JL: Targeting autophagy augments the anticancer activity of the histone deacetylase inhibitor SAHA to overcome Bcr-Abl-mediated drug resistance. Blood 110: 313-322, 2007.
55. Rosenfeld MR, Ye X, Supko JG, Desideri S, Grossman SA, Brem S, Mikkelson T, Wang D, Chang YC, Hu J, *et al*: A phase I/II trial of hydroxychloroquine in conjunction with radiation therapy and concurrent and adjuvant temozolomide in patients with newly diagnosed glioblastoma multiforme. Autophagy 10: 1359-1368, 2014.
56. Das G, Shravage BV and Baehrecke EH: Regulation and function of autophagy during cell survival and cell death. Cold Spring Harb Perspect Biol 4: pii: 008813, 2012.
57. Navarro-Yepes J, Burns M, Anandhan A, Khalimonchuk O, del Razo LM, Quintanilla-Vega B, Pappa A, Panayiotidis MI and Franco R: Oxidative stress, redox signaling, and autophagy: Cell death versus survival. Antioxid Redox Signal 21: 66-85, 2014.
58. Gong C, Song E, Codogno P and Mehrpour M: The roles of BECN1 and autophagy in cancer are context dependent. Autophagy 8: 1853-1855, 2012.
59. White E: Deconvoluting the context-dependent role for autophagy in cancer. Nat Rev Cancer 12: 401-410, 2012.
60. White E: The role for autophagy in cancer. J Clin Invest 125: 42-46,2015.